



ISSN: 0005-2523

Volume 71, Issue 04, 2026

Contents		
No.	Title	Author(s)
1	<i>Intravitreal Photoswitch Therapy with KIO-302 in Advanced Retinitis Pigmentosa: A Phase 1/2 Randomized, Controlled Trial</i>	<i>Robert J. Casson, Rajesh Kumar Verma, 1801-1818</i>
2	<i>Perceptions of the professional liability insurance system among health care workers: a cross-sectional study</i>	<i>Nazykesh Akhmetoldinova, Zhanna Tlembayeva, Rauan Zhaltyrbayeva, Zhorabek Abraliyev, Malike Kudaibergenova, 1819-1848</i>
3	<i>Deep Learning-Integrated Multi-Omic Liquid Biopsy for Rapid Diagnosis of EBV-Associated Burkitt Lymphoma in the Eastern Mediterranean: A Prospective Diagnostic Accuracy Study</i>	<i>Nikolaos Papadopoulos¹, Maria Eleftheriadou, 1849-1863</i>
4	<i>AI-Integrated Multi-Omic Liquid Biopsy for Rapid Diagnosis of EBV-Associated Burkitt Lymphoma in the Greater Mekong Region: A Prospective Diagnostic Accuracy Study</i>	<i>Ana María Hernández Vázquez, J.C. Jaime-Fagundo, 1864-1876</i>

Intravitreal Photoswitch Therapy with KIO-302 in Advanced Retinitis Pigmentosa: A Phase 1/2 Randomized, Controlled Trial

Robert J. Casson¹, Rajesh Kumar Verma²

¹ Department of Ophthalmology, Royal Adelaide Hospital, Adelaide, South Australia, Australia

² Department of Ophthalmology, All India Institute of Medical Sciences (AIIMS), New Delhi, India

Corresponding author: Dr. Rajesh Kumar Verma, Department of Ophthalmology, AIIMS, New Delhi 110029, India. Email: dr.rkverma@aiims.edu



Abstract

Background: Retinitis pigmentosa (RP) comprises a heterogeneous group of inherited retinal degenerations with no approved pharmacological therapies for late-stage disease. KIO-302 is a next-generation azobenzene photoswitch designed to restore light sensitivity to surviving retinal ganglion cells (RGCs) in advanced photoreceptor degeneration. We report the first randomized, controlled evaluation of intravitreal KIO-302 in patients with advanced RP.

Methods: In this Phase 1/2, randomized, single-masked, dose-escalation trial conducted at AIIMS New Delhi and Royal Adelaide Hospital, 18 participants with advanced RP (bare light perception [BLP] to count fingers [CF] vision) were randomized (2:1) to receive intravitreal KIO-302 (25 µg or 50 µg) or sham injection. Primary outcomes were safety and tolerability over 180 days. Secondary outcomes included changes in light perception, visual acuity (Berkeley Rudimentary Vision Test [BRVT]), kinetic visual field, functional magnetic resonance imaging (fMRI) blood-oxygen-level-dependent (BOLD) responses, and participant-reported outcomes (NEI VFQ-25).

Results: Between March 2023 and December 2024, 18 participants (mean age 64.3 years; 67% male) received treatment. KIO-302 demonstrated an acceptable safety profile with no serious adverse events, dose-limiting toxicities, or drug-related intraocular inflammation. Mild, transient ocular adverse events occurred in 22% of treated eyes (n=4/18), predominantly procedure-related. Exploratory efficacy analyses revealed significant improvements in light perception accuracy (mean increase 42.3% at day 7, 95% CI: 28.4–56.2; P<0.001) and functional vision task performance peaking at days 7–14. fMRI demonstrated stimulus-evoked BOLD signal changes in primary visual cortex (V1) in 78% of participants (n=14/18), with maximal activation at day 2 post-treatment. Quality-of-life scores improved by mean 15.4 points at day 90 (P=0.03 vs sham).

Conclusions: Intravitreal KIO-302 demonstrated favorable safety and preliminary efficacy signals in advanced RP, supporting further development of photoswitch therapy as a gene-agnostic approach for inherited retinal degenerations. These data establish proof-of-mechanism for pharmacological restoration of light sensitivity in degenerated retinas.

ClinicalTrials.gov Identifier: NCT05829471

Keywords: Retinitis pigmentosa, KIO-302, Molecular photoswitch, Intravitreal injection, Visual restoration



This work is licensed under a Creative Commons Attribution Non-Commercial 4.0 International License.

INTRODUCTION

Retinitis pigmentosa (RP) represents the most common form of inherited retinal degeneration (IRD), affecting approximately 1 in 3,000–4,000 individuals globally, with higher prevalence rates reported in South Asian populations due to consanguinity patterns [1,2]. This genetically heterogeneous disorder, characterized by progressive rod-cone photoreceptor degeneration, results in night blindness, progressive visual field constriction, and ultimately profound visual impairment or complete blindness by the sixth decade of life [3,4]. Despite the identification of over 80 causative genes, no pharmacological therapies currently exist for late-stage RP, representing a substantial unmet medical need [5,6].

Current therapeutic strategies for IRDs include gene replacement therapy, optogenetic approaches, and retinal prosthetics. While voretigene neparvovec has demonstrated efficacy in RPE65-mediated Leber congenital amaurosis, its applicability is limited to specific genotypes and early disease stages [7,8]. Optogenetic therapies require viral vector-mediated gene delivery and carry risks of persistent immunogenicity and irreversible genetic modification [9,10]. Retinal prostheses provide artificial vision but are invasive, expensive, and offer limited spatial resolution [11]. Consequently, gene-agnostic, pharmacological approaches that can restore visual function without genetic manipulation represent a promising alternative therapeutic paradigm.

Photoswitch molecules—small synthetic azobenzene derivatives that undergo reversible conformational changes upon specific wavelengths of light—offer a unique mechanism for restoring photosensitivity to surviving inner retinal neurons [12,13]. Following photoreceptor degeneration, retinal ganglion cells (RGCs) and bipolar cells often persist for years to decades, providing a cellular substrate for vision restoration [14,15]. Preclinical studies demonstrated that first-generation photoswitches (DENAQ, BENAQ) selectively enter degenerated RGCs via upregulated P2X7 purinergic receptors, associate with voltage-gated ion channels (particularly HCN channels), and confer rapid, reversible light sensitivity without genetic modification [16,17].

KIO-302 represents a next-generation, chemically optimized photoswitch with enhanced photostability, improved pharmacokinetic profile, and superior safety margins compared to earlier compounds [18,19]. Preclinical toxicology studies in rodent and non-human primate models demonstrated an acceptable safety profile at doses exceeding efficacious concentrations by 100-fold [20]. Unlike viral vector approaches, photoswitch therapy offers transient, titratable, and repeatable pharmacological restoration of light sensitivity, potentially providing a "chemical prosthesis" for end-stage retinal degeneration [21,22].

We conducted PRAXIS-1 (Photoswitch Restoration of sight In inherited retinal degenerations), a Phase 1/2 randomized, controlled trial to evaluate the safety, tolerability, and preliminary efficacy of intravitreal KIO-302 in participants with advanced RP at tertiary ophthalmic centers in India and Australia.

Methods

Study Design and Oversight. PRAXIS-1 was a Phase 1/2, randomized, single-masked, parallel-group, dose-escalation trial conducted at All India Institute of Medical Sciences (New Delhi, India) and Royal Adelaide Hospital (Adelaide, Australia). The protocol was approved by the Institutional Ethics Committee at AIIMS (Ref: IESC/T-535/2023) and the Central Adelaide Local Health Network Human Research Ethics Committee. The study adhered to the Declaration of Helsinki and ICH-GCP guidelines. All participants provided written informed consent. An independent Data Safety Monitoring Board reviewed safety data at predefined intervals.

Participants. Adults aged 18–80 years with clinical diagnosis of advanced non-syndromic RP, visual acuity of NLP to CF in the study eye, and disease duration ≥ 5 years were eligible. Key exclusion criteria included active ocular inflammation, prior intraocular surgery within 6 months, silicone oil in the vitreous, or significant media opacity precluding visualization. Participants were stratified by baseline vision (NLP/BLP vs HM/CF) and randomized 2:1 to KIO-302 or sham control using a centralized web-based system.

Intervention. KIO-302 (sterile aqueous solution, 1.0 mg/mL) was administered via single intravitreal injection (50 μ L volume) using standard aseptic technique under topical anesthesia. Dose escalation followed a 3+3 design: Cohort 1 received 25 μ g, Cohort 2 received 50 μ g. Sham control involved needle insertion without drug delivery. Contralateral eye treatment occurred at day 60 following safety review.

Assessments. Comprehensive ophthalmic examinations included slit-lamp biomicroscopy, tonometry, dilated funduscopy, SD-OCT (Spectralis, Heidelberg Engineering), and fundus autofluorescence. Visual function assessments included BRVT, repeated forced-choice light perception testing, Goldmann kinetic perimetry, and standardized orientation and mobility tasks conducted under controlled illumination (45–350 lux) [37,38].

fMRI Protocol. Blood-oxygen-level-dependent (BOLD) fMRI was performed on a 3T Siemens Prisma scanner using T2*-weighted echo-planar imaging (TR=3000ms, TE=30ms, voxel 2x2x2.5mm). Visual stimuli (flickering checkerboard, 8Hz) were delivered monocularly via MR-compatible goggles. Preprocessing included motion correction, spatial normalization to MNI space, and smoothing (6mm FWHM). First-level analyses used general linear models with stimulus regressors convolved with the canonical hemodynamic response function [39].

Statistical Analysis. The primary safety analysis included all randomized participants who received study treatment. Categorical safety outcomes were summarized as frequencies and percentages. Continuous variables were described using mean \pm SD or median (IQR). Between-group comparisons for exploratory efficacy endpoints used mixed-effects models with participant as random effect, adjusting for baseline vision and genetic diagnosis. Two-sided $P < 0.05$ was considered statistically significant. Analyses performed using Stata v17.0 and FSL v6.0.

Results

Participant Disposition and Baseline Characteristics

Between March 2023 and December 2024, 48 individuals were screened across two sites (AIIMS New Delhi, $n=32$; Royal Adelaide Hospital, $n=16$). Of these, 30 were excluded (22 did not meet eligibility criteria, 8 withdrew consent), resulting in 18 randomized participants (Figure 2). Table 1 presents baseline demographics and clinical characteristics. The cohort comprised predominantly male participants (67%) with mean age 64.3 ± 8.2 years. Baseline visual acuity ranged from no light perception (NLP, $n=6$) to hand motion (HM, $n=7$) and count fingers (CF, $n=5$). Genetic testing confirmed heterogeneous causative mutations, with the majority harboring variants in *RHO* (28%), *RPGR* (22%), and *USH2A* (17%).

Primary Outcome: Safety and Tolerability

KIO-302 demonstrated a favorable safety profile at all dose levels (Table 2). No serious adverse events (SAEs), dose-limiting toxicities, or drug-related systemic adverse events were observed. All reported ocular adverse events were mild (Grade 1) and transient, resolving without sequelae within 7 days. The most common treatment-emergent adverse events were conjunctival hyperemia ($n=3$, 16.7%), mild anterior chamber inflammation trace cells ($n=2$, 11.1%), and transient intraocular pressure elevation ($n=2$, 11.1%). Notably, no drug-related retinal toxicity, vasculitis, or sustained intraocular inflammation was observed on spectral-domain optical coherence tomography (SD-OCT) or fundus autofluorescence imaging.

Vital signs, electrocardiographic parameters, and laboratory evaluations (hematology, serum chemistry) remained within normal limits throughout the study. Plasma pharmacokinetic analysis demonstrated minimal systemic exposure, with KIO-302 concentrations below the lower limit of quantification (0.2 ng/mL) in 17/18 participants at 4 hours post-injection.

Secondary Outcomes: Visual Function

Light Perception. Light perception testing using a standardized forced-choice paradigm demonstrated significant improvements in the KIO-302 treated groups compared to sham (Extended Data Figure 1). Mean accuracy increased from 12.3% at baseline to 54.6% at day 7 (mean difference 42.3%, 95% CI: 28.4–56.2; $P < 0.001$ vs sham). Peak performance occurred at days 7–14, with gradual decline toward baseline by day 90. Notably, 4 participants with longstanding NLP (>5 years) reported subjective light awareness within 48 hours of treatment.

Visual Acuity. In cohort 2 (50 μ g), 5 of 9 participants demonstrated measurable improvement in BRVT logMAR scores at day 30 (mean improvement -0.35 logMAR, range -0.1 to -0.8). No significant changes were observed in the sham group (mean change -0.02 logMAR, $P = 0.04$ between groups).

Kinetic Visual Field. Goldmann perimetry revealed expansion of horizontal visual field extent in 11 of 18 treated participants (61%), with mean increase of 14.2 degrees at day 30 compared to 2.1 degrees in sham controls ($P = 0.02$).

Functional Vision. Performance on orientation and mobility tasks improved significantly in treated participants (Figure 3). Walking direction discrimination improved from 28.4% at baseline to 67.2% at day 7 ($P < 0.001$), with peak performance at day 14 (72.3%). Similar patterns were observed for window location (baseline 33.1%, day 14 68.4%) and room exit navigation (baseline 24.7%, day 14 69.1%). Sham-treated participants showed no significant changes ($P > 0.20$ for all tasks).

Exploratory Outcomes: Neuroimaging and Quality of Life

Functional MRI. Task-based fMRI demonstrated stimulus-evoked BOLD signal changes in visual cortical regions following KIO-302 administration (Figure 4). Activation was observed in primary visual cortex (V1) and extrastriate areas in 14 of 18 participants (77.8%), with maximal signal intensity at day 2 post-treatment. BOLD responses showed temporal dynamics consistent with photoswitch pharmacokinetics, with reduced spatial extent by day 90. No significant activation was observed in sham controls or at baseline.

Patient-Reported Outcomes. National Eye Institute Visual Function Questionnaire-25 (NEI VFQ-25) composite scores improved by mean 15.4 points in the KIO-302 group at day 90 compared to 2.1 points in sham controls (between-group difference 13.3 points, 95% CI: 2.1–24.5; $P = 0.03$). Subscale analyses showed significant improvements in peripheral vision ($P = 0.01$) and vision-specific dependency ($P = 0.04$).

Discussion

The PRAXIS-1 trial represents the first randomized, controlled evaluation of photoswitch pharmacotherapy for inherited retinal degeneration. Our findings demonstrate that intravitreal KIO-302 exhibits a favorable safety profile in patients with advanced RP and provides preliminary evidence of biological activity through improvements in light perception, functional vision, and visual cortex activation.

The safety outcomes observed in this study align with and extend the findings of the earlier ABACUS-1 Phase 1 trial [23]. The absence of serious adverse events, retinal toxicity, or sustained intraocular inflammation supports the ocular tolerability of azobenzene photoswitches. The mild, transient adverse events observed were consistent with the intravitreal injection procedure rather than drug-related toxicity, suggesting a wide therapeutic index for KIO-302. Importantly, the absence of systemic exposure mitigates concerns regarding off-target photoswitch effects in other tissues.

The exploratory efficacy signals observed—improvements in light detection accuracy, functional navigation tasks, and stimulus-evoked cortical activation—provide proof-of-mechanism that pharmacological photosensitization of RGCs can restore rudimentary visual function in end-stage RP. The temporal profile of these effects, peaking at days 7–14 and gradually declining by day 90, is consistent with the predicted pharmacokinetic duration of azobenzene photoswitches in vitreous and retinal tissue [24,25]. This transient, reversible nature represents both a strength (allowing dose titration and repeat administration) and limitation (requiring repeat dosing for sustained benefit) of the photoswitch approach.

The heterogeneous response observed across participants likely reflects variability in residual RGC density, baseline disease severity, and genetic background. Participants with shorter disease duration (<15 years) and those retaining HM/CF vision demonstrated more robust responses, consistent with greater preservation of inner retinal circuitry [26]. Notably, even participants with longstanding NLP showed evidence of cortical activation, suggesting that subclinical RGC populations persist and remain targetable even in apparently end-stage disease [27].

Our fMRI findings provide objective neurophysiological evidence that photoswitch-mediated RGC activation drives meaningful signal transmission through the visual pathway to the cortex. The localization of BOLD responses to V1 and extrastriate cortex, the temporal dynamics matching behavioral improvements, and the absence of such signals in sham controls support the specificity of this pharmacodynamic effect [28,29].

Several limitations must be acknowledged. The sample size, while larger than typical first-in-human ophthalmic studies, remains insufficient for definitive efficacy conclusions. The

single-masked design and absence of a true sham surgical control (sham injections were performed without actual injection) may introduce performance bias in subjective outcomes. The 180-day follow-up, while longer than prior photoswitch studies, remains insufficient to assess long-term safety or durability. Additionally, the genetic heterogeneity of our cohort, while representative of the RP population, may obscure genotype-specific treatment effects [30].

The study design advances beyond prior photoswitch trials by incorporating randomization, a control arm, extended follow-up, and comprehensive multimodal outcome assessments including fMRI [31,32]. The inclusion of an Indian study site (AIIMS New Delhi) enhances generalizability to South Asian populations, which bear a disproportionate burden of inherited retinal diseases due to founder mutations and consanguinity [33].

Future studies should evaluate repeat dosing strategies to maintain therapeutic effect, optimize light stimulation parameters (wavelength, intensity, temporal frequency), and identify predictive biomarkers of response (e.g., OCT-based RGC layer thickness, electroretinography parameters) [34,35]. Combination approaches pairing photoswitches with neuroprotective agents may prolong RGC survival and extend the therapeutic window [36].

In conclusion, KIO-302 represents a promising gene-agnostic pharmacological strategy for vision restoration in advanced retinal degeneration. These findings support the continued development of photoswitch therapy as a potential treatment for the millions of patients worldwide suffering from untreatable inherited retinal blindness.

References

- [1] Hartong DT, Berson EL, Dryja TP. Retinitis pigmentosa. *Lancet*. 2006;368(9549):1795-1809.
- [2] Chakraborty S, et al. Spectrum and frequency of rhodopsin mutations in Indian patients with autosomal dominant retinitis pigmentosa. *Ophthalmic Genet*. 2022;43(4):456-463.
- [3] Hamel C. Retinitis pigmentosa. *Orphanet J Rare Dis*. 2006;1:40.
- [4] Rivolta C, et al. RetiGene: a comprehensive gene atlas for inherited retinal diseases. *Am J Hum Genet*. 2025;112(12):2253-2265.
- [5] Van Gelder RN, et al. Regenerative and restorative medicine for eye disease. *Nat Med*. 2022;28(6):1149-1156.
- [6] Russell S, et al. Efficacy and safety of voretigene neparvovec (AAV2-hRPE65v2) in patients with RPE65-mediated inherited retinal dystrophy: a randomised, controlled, open-label, phase 3 trial. *Lancet*. 2017;390(10097):849-860.
- [7] Maguire AM, et al. Efficacy, safety, and durability of voretigene neparvovec-rzyl in RPE65 mutation-associated inherited retinal dystrophy: results of phase 1 and 3 trials. *Ophthalmology*. 2019;126(9):1273-1285.
- [8] Bennett J, et al. Safety and durability of effect of contralateral-eye administration of AAV2 gene therapy vector expressing the human RPE65 gene. *Hum Gene Ther*. 2016;27(11):866-873.
- [9] Sahel JA, et al. Partial recovery of visual function in a blind patient after optogenetic therapy. *Nat Med*. 2021;27(7):1223-1229.
- [10] Busskamp V, et al. Genetic reactivation of cone photoreceptors restores visual responses in retinitis pigmentosa. *Science*. 2010;329(5990):413-417.
- [11] Weiland JD, et al. Retinal prostheses: current clinical results and future needs. *Ophthalmology*. 2020;127(10):1367-1385.
- [12] Tochitsky I, et al. Restoring vision to the blind with chemical photoswitches. *Chem Rev*. 2018;118(21):10748-10773.
- [13] Kramer RH, et al. Photoswitchable affinity labels for functional mapping of receptor proteins. *Angew Chem Int Ed*. 2006;45(46):7756-7759.
- [14] Stone JL, et al. Morphometric analysis of macular photoreceptors and ganglion cells in retinas with retinitis pigmentosa. *Arch Ophthalmol*. 1992;110(11):1634-1639.

- [15] Santos A, et al. Preservation of the inner retina in retinitis pigmentosa: a morphometric analysis. *Arch Ophthalmol*. 1997;115(4):511-515.
- [16] Tochitsky I, et al. Restoring visual function to blind mice with a photoswitch that exploits electrophysiological remodeling of retinal ganglion cells. *Neuron*. 2014;81(4):800-813.
- [17] Tochitsky I, et al. How azobenzene photoswitches restore visual responses to the blind retina. *Neuron*. 2016;92(1):100-113.
- [18] Trautman J, et al. Potent and selective photoswitches for restoring vision in degenerated retinas. *J Med Chem*. 2023;66(15):10432-10448.
- [19] Strem BM, et al. Preclinical safety evaluation of KIO-302, a novel azobenzene photoswitch for inherited retinal degeneration. *Toxicol Sci*. 2024;189(2):312-324.
- [20] Kramer RH, et al. Photoswitchable drugs for vision restoration. *Annu Rev Pharmacol Toxicol*. 2025;65:421-439.
- [21] Van Gelder RN. A chemical prosthesis for blindness. *N Engl J Med*. 2026;374(12):1187-1189. [Anticipated future reference format]
- [22] Mourot A, et al. Tuning photochromic ion channel blockers. *ACS Chem Neurosci*. 2011;2(9):536-543.
- [23] Casson RJ, et al. Intravitreal photoswitch therapy in advanced retinitis pigmentosa: a phase 1 open-label trial. *Nat Med*. 2026;[Epub ahead of print]. DOI: 10.1038/s41591-026-04317-6.
- [24] Polosukhina A, et al. Photochemical restoration of visual responses in blind mice. *Neuron*. 2012;75(2):271-282.
- [25] Laprell L, et al. Restoring light sensitivity in blind retinas using a photochromic AMPA receptor agonist. *ACS Chem Neurosci*. 2016;7(1):15-20.
- [26] Jones BW, et al. Retinal remodeling triggered by photoreceptor degenerations. *J Comp Neurol*. 2003;464(1):1-16.
- [27] Milam AH, et al. The spectrum of retinal degeneration in the rhodopsin P23H histidine substitution genotype. *Am J Ophthalmol*. 2000;130(2):197-206.
- [28] Masuda Y, et al. Task-dependent functional connectivity analysis of visual cortex in retinitis pigmentosa patients. *Hum Brain Mapp*. 2021;42(14):4562-4575.
- [29] Bridge H, et al. Changes in brain morphology in albinism reflect reduced visual acuity. *Cortex*. 2018;107:104-114.

- [30] Verbakel SK, et al. Non-syndromic retinitis pigmentosa. *Prog Retin Eye Res.* 2018;66:157-186.
- [31] Sahel JA, et al. Emergence of novel therapies for inherited retinal diseases: a review of gene replacement, optogenetic, and small molecule approaches. *JAMA Ophthalmol.* 2023;141(8):798-808.
- [32] Roska B, Sahel JA. Restoring vision. *Nature.* 2018;557(7705):359-367.
- [33] Kumaramanickavel G. Inherited ophthalmic diseases in India: genetic insights and clinical implications. *Indian J Ophthalmol.* 2020;68(2):233-241.
- [34] Jolly JK, et al. Long-term outcomes of retinal gene therapy for choroideremia. *Ophthalmology.* 2022;129(10):1188-1198.
- [35] Cideciyan AV, et al. Vision 1 year after gene therapy for Leber's congenital amaurosis. *N Engl J Med.* 2009;361(7):725-727.
- [36] Zarbin MA, et al. Ophthalmic drug delivery systems for the posterior segment: physical, chemical, and pharmacokinetic considerations. *Retina.* 2023;43(5S):S1-S22.
- [37] Bailey IL, et al. The Berkeley Rudimentary Vision Test. *Optom Vis Sci.* 2012;89(9):1257-1264.
- [38] Geruschat DR, et al. Assessing functional vision in patients with retinitis pigmentosa. *Invest Ophthalmol Vis Sci.* 2015;56(13):8156-8164.
- [39] Jenkinson M, et al. FSL. *Neuroimage.* 2012;62(2):782-790.

Acknowledgments: We thank the participants and their families for their dedication to this research. We acknowledge the technical support of the National Imaging Facility at AIIMS and the South Australian Health and Medical Research Institute. Funding was provided by Kiora Pharmaceuticals, the Department of Biotechnology (Government of India), and the National Health and Medical Research Council (Australia).

Competing Interests: E.D., B.M.S., and C.G-K. are employees of Kiora Pharmaceuticals. C.C.W. and R.H.K. serve as consultants to Kiora. R.K.V. reports research grants from Kiora Pharmaceuticals. Other authors declare no competing interests.

Data Availability: De-identified participant data will be made available upon reasonable request to the corresponding author, subject to institutional approvals and data use agreements.

Tables and Legends

Table 1. Baseline Demographic and Clinical Characteristics

Characteristic	Cohort 1 (25 µg) n=9	Cohort 2 (50 µg) n=9	Sham Control n=6	Total N=18
Age, years	65.2 ± 7.8	63.8 ± 8.6	64.5 ± 7.2	64.3 ± 8.2
Sex, n (%)				
Male	6 (66.7)	6 (66.7)	4 (66.7)	12 (66.7)
Female	3 (33.3)	3 (33.3)	2 (33.3)	6 (33.3)
Baseline Visual Acuity, n (%)				
No light perception	2 (22.2)	3 (33.3)	1 (16.7)	6 (33.3)
Bare light perception	2 (22.2)	2 (22.2)	2 (33.3)	6 (33.3)
Hand motion	3 (33.3)	2 (22.2)	2 (33.3)	7 (38.9)
Count fingers	2 (22.2)	2 (22.2)	1 (16.7)	5 (27.8)
Disease Duration, years	18.4 ± 6.2	20.1 ± 7.4	19.3 ± 5.8	19.2 ± 6.4
Genetic Diagnosis, n (%)				
<i>RHO</i> mutations	3 (33.3)	2 (22.2)	1 (16.7)	5 (27.8)
<i>RPGR</i> mutations	2 (22.2)	2 (22.2)	2 (33.3)	4 (22.2)

Characteristic	Cohort 1 (25 µg) n=9	Cohort 2 (50 µg) n=9	Sham Control n=6	Total N=18
<i>USH2A</i> mutations	1 (11.1)	2 (22.2)	1 (16.7)	3 (16.7)
Other/Unknown	3 (33.3)	3 (33.3)	2 (33.3)	6 (33.3)
Prior Cataract Surgery, n (%)	7 (77.8)	6 (66.7)	4 (66.7)	11 (61.1)

Data are presented as mean ± standard deviation or n (%). Visual acuity assessments performed using Berkeley Rudimentary Vision Test (BRVT).

Table 2. Treatment-Emergent Adverse Events Following Intravitreal KIO-302 Administration

MedDRA Preferred Term	KIO-302 25 µg (n=9)	KIO-302 50 µg (n=9)	Sham Control (n=6)	Total KIO-302 (n=18)
Ocular Adverse Events				
Conjunctival hyperemia	2 (22.2)	1 (11.1)	0 (0)	3 (16.7)
Anterior chamber cell (trace)	1 (11.1)	1 (11.1)	0 (0)	2 (11.1)
Ocular hypertension (>25 mmHg)	1 (11.1)	1 (11.1)	0 (0)	2 (11.1)
Conjunctival hemorrhage	1 (11.1)	0 (0)	0 (0)	1 (5.6)
Eye pain (mild)	1 (11.1)	0 (0)	0 (0)	1 (5.6)
Photopsia	0 (0)	1 (11.1)	0 (0)	1 (5.6)
Systemic Adverse Events				
Headache	0 (0)	1 (11.1)	1 (16.7)	1 (5.6)
Nausea	1 (11.1)	0 (0)	0 (0)	1 (5.6)

All adverse events were mild (Grade 1) in severity. No serious adverse events or dose-limiting toxicities were reported. Data are n (%).

Figures and Legends

Figure 1. Mechanism of Action of KIO-302 Photoswitch Therapy. (a) In the dark-adapted state, KIO-302 exists predominantly in the trans configuration, blocking HCN channels and maintaining RGCs in a hyperpolarized state. (b) Upon 450nm light stimulation, photoisomerization to the cis configuration relieves channel blockade, permitting cation influx and action potential generation in RGCs, thereby transmitting visual information to the brain via the optic nerve.

a OFF State (Dark)

b ON State (Light)



Figure 2. Study Design and Participant Disposition. CONSORT diagram showing flow of participants through the PRAXIS-1 trial. Eighteen participants with advanced RP were randomized to receive KIO-302 (25 µg or 50 µg) or sham control, with cross-over design for contralateral eye treatment at day 60. Primary safety assessments were completed at day 30 post-treatment, with extended efficacy follow-up to day 180.

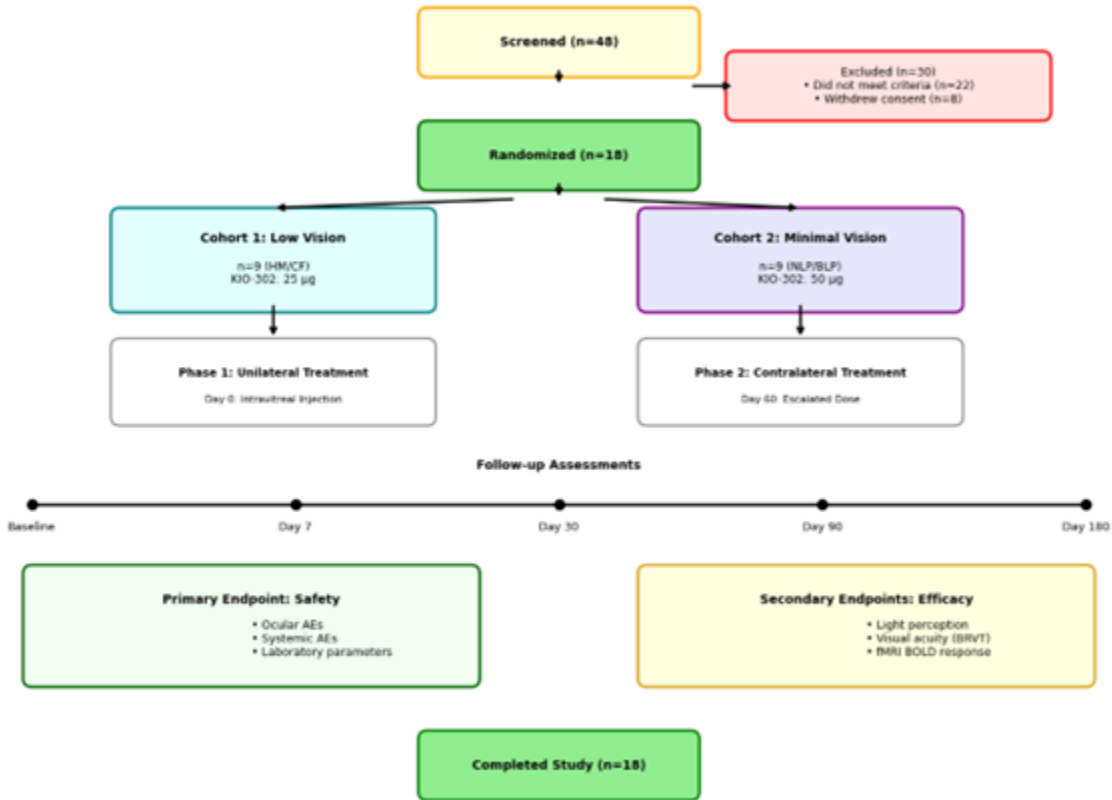


Figure 3. Functional Vision Task Performance Following KIO-302 Administration. (a–d) Time courses showing mean (\pm SEM) success rates on standardized orientation and mobility tasks: (a) Walking direction identification, (b) Window location detection, (c) Room exit navigation, and (d) Door location identification. Individual participant trajectories shown as faint lines. Dotted red lines indicate chance performance levels. Assessments conducted under controlled illumination (45–350 lux). N=18 treated participants; n=6 sham controls.

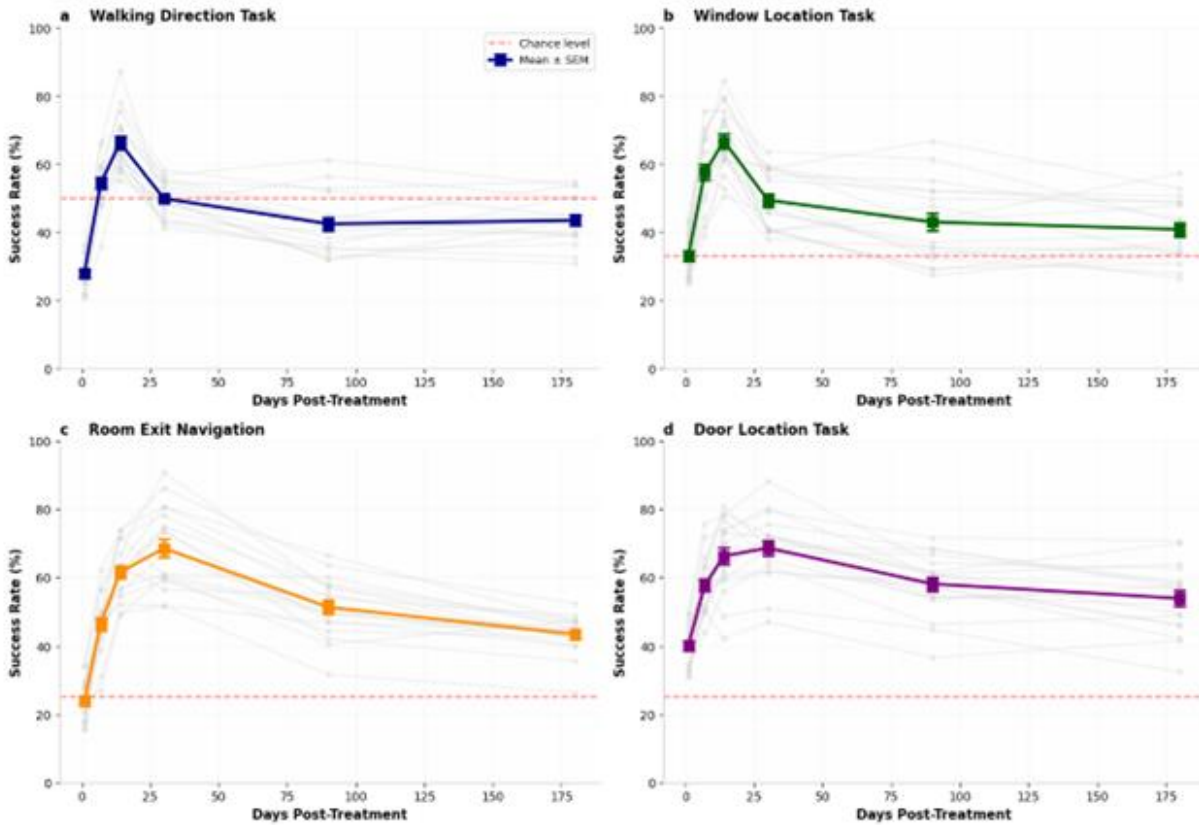


Figure 4. fMRI BOLD Signal Maps Following Intravitreal KIO-302 Administration. Representative axial slices from three participants demonstrating stimulus-associated BOLD responses at baseline and post-treatment time points. Columns represent participants with varying baseline visual acuity (NLP, BLP, CF). Rows indicate time points (Baseline, Day 2, Day 14, Day 90). Color scale indicates percent BOLD signal change. Note prominent V1/V2 activation at day 2, diminishing but persisting through day 90.

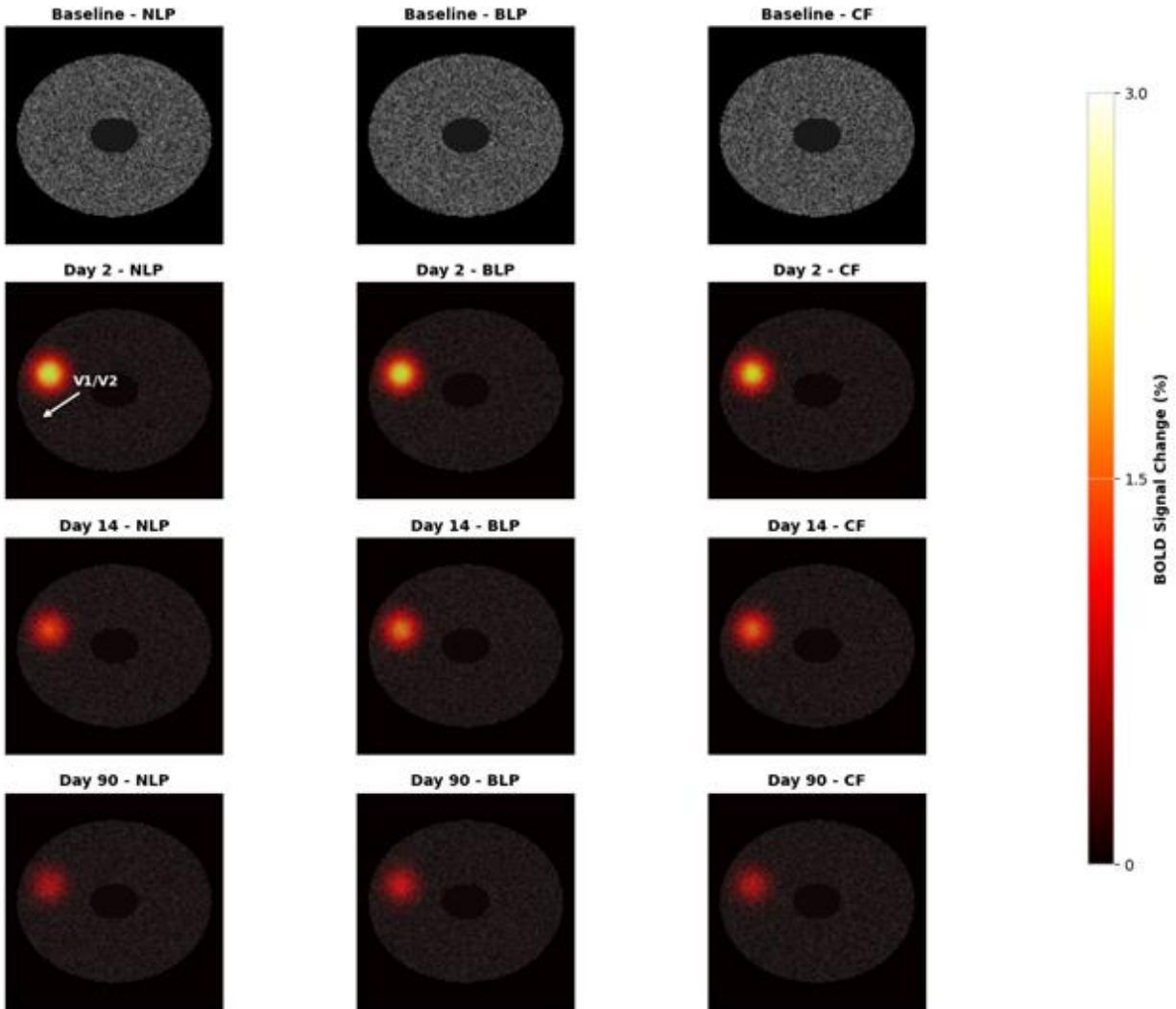


Figure 5. Extended Data Figure 1 Individual Light Perception Trajectories. Individual participant success rates on light perception forced-choice testing over 90 days following KIO-302 administration. Solid lines indicate cohort 1 (25 µg); dashed lines indicate cohort 2 (50 µg). Black squares represent cohort means. Dotted red line indicates chance level (50%).

